**Table S1** List of 22 *R. pseudosolanacearum* Ps29 *mcp* genes and their deletion mutants

| *mcp* No. | Gene[a] | Mutant strain[b] | Number of amino acids | | Identity (%)[c] | Accession No. |
|---|---|---|---|---|---|---|
| | | | GMI1000 | Ps29 | | |
| 01 | RSc0606 | DPS01 | 617 | 617 | 100 | LC005226 |
| 02 | RSc1155 | DPS02 | 629 | 629 | 99 | LC005227 |
| 03 | RSc1156 | DPS03 | 600 | 600 | 99 | LC005228 |
| 04 | RSc1234 | DPS04 | 514 | 514 | 100 | LC005229 |
| 05 | RSc1460 | DPS05 | 513 | 513 | 99 | LC005230 |
| 06 | RSc1894 | DPS06 | 535 | 535 | 99 | LC005231 |
| 07 | RSc1950 | DPS07 | 329 | 329 | 99 | LC005232 |
| 08 | RSc2799 | DPS08 | 515 | 515 | 99 | LC005233 |
| 09 | RSc3136 | DPS09 | 661 | 661 | 99 | LC005234 |
| 10 | RSc3307 | DPS10 | 646 | 646 | 99 | LC005235 |
| 11 | RSc3412 (*cheD4*) | DPS11 | 515 | 515 | 99 | LC005236 |
| 12 | RSc0671 (*pilJ*) | DPS12 | 743 | 743 | 99 | LC005237 |
| 13 | RSp0255 | DPS13 | 529 | 529 | 99 | LC005238 |
| 14 | RSp0507 (*cheD1*) | DPS14 | 600 | 600 | 99 | LC005239 |
| 15 | RSp0840 | DPS15 | 518 | 518 | 99 | LC005240 |
| 16 | RSp0303 (*cheD2*) | DPS16 | 515 | 515 | 99 | LC005241 |
| 17 | RSp1027 | DPS17 | 524 | 524 | 99 | LC005242 |
| 18 | RSp1099 | DPS18 | 513 | 513 | 100 | LC005243 |
| 19 | RSp1209 | DPS19 | 524 | 524 | 99 | LC005244 |
| 20 | RSp1224 (*aer*) | DPS20 | 514 | 514 | 99 | LC005245 |
| 21 | RSp1363 | DPS21 | 543 | 543 | 99 | LC005246 |
| 22 | RSp1406 (*cheD3*) | DPS22 | 608 | 608 | 99 | LC005247 |

[a] Gene name designations in parentheses indicate gene name based on the annotated GMI1000 genome sequence.

[b] Strain names of *R. pseudosolanacearum* Ps29 *mcp* deletion mutants.

[c] Identity between amino acid sequences of GMI1000 and Ps29 orthologs.

**Table S2** Accession numbers of genome sequences of the *R. solanacearum* species complex

| Strain | Accession number | |
|---|---|---|
| | Chromosome | Mega plasmid |
| *R. solanacearum* CFBP2957 | NC_014307.1 | NC_014309.1 |
| *R. solanacearum* Po82 | NC_0.17574.1 | NC_017575.1 |
| *R. pseudosolanacearum* GMI1000 | NC_003295.1 | NC_003296.1 |
| *R. pseudosolanacearum* FQY4 | NC_020799.1 | NC_021745.1 |
| *R. pseudosolanacearum* CMR15 | NC_017559.1 | NC_017589.1 |
| *R. syzygii* subsp. *indonesiensis* PSI07 | FP885906.2 | FP885891.2 |

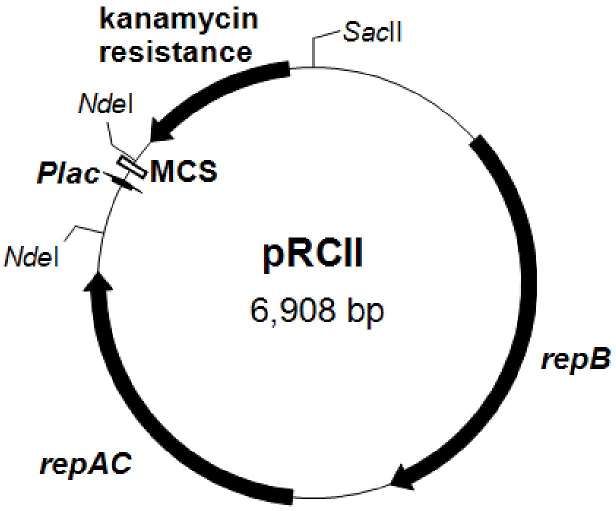

**Fig. S1** Physical map of pRCII. The region between *Sac*II and *Nde*I including *repABC* was amplified from pKZ27. The region of kanamycin resistant gene was amplified from pUC4K. The region between *Nde*I sites including *lac* promoter and multiple cloning site (MCS) was amplified from pUCP18.

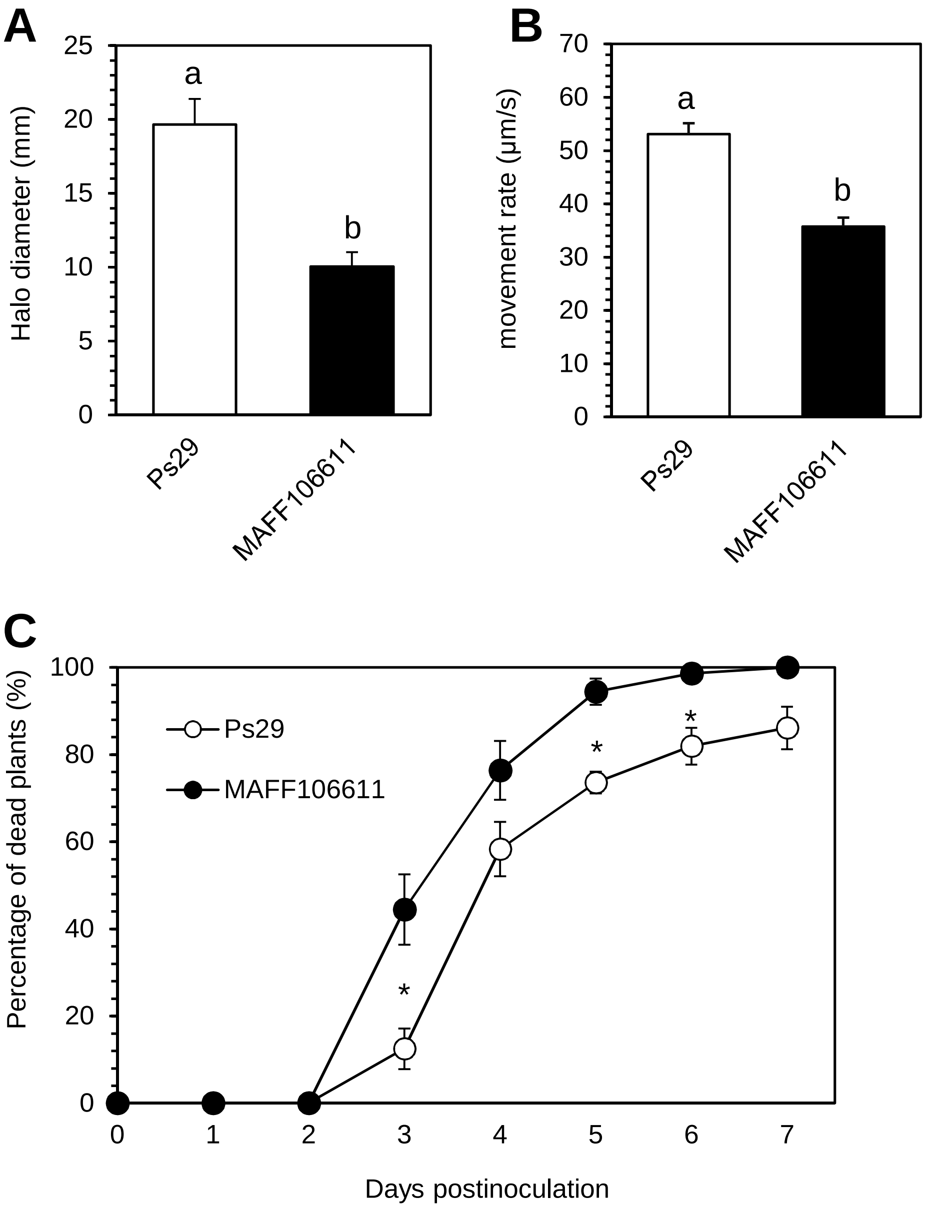

**Fig. S2** Motility and virulence of *R. pseudosolanacearum* Ps29 and MAFF106611. **A**, Swimming assay in semi-solid agar plates. Bacterial cells were inoculated into semi-solid agar plates containing 1 g/l Tryptone, 5 g/l KCl, and 3 g/l agarose and incubated at 28˚C. After 3 days, halo diameter was measured. Vertical bars represent the standard errors of measurements done in six independent experiments. Different letters indicate significant difference (Student's *t*-test, $P < 0.05$). **B**, Microscope observation. Bacterial cells were observed by microscope and movement rate of cells were measured. Vertical bars represent the standard errors of measurements done about 30 cells in three independent experiments. Different letters indicate significant difference (Student's *t*-test, $P < 0.05$). **C**, Virulence assay by root-dip inoculation. Bacterial cells were inoculated 7-day-old wounded tomato seedling by dipping root-tip into cell suspension. In each experiment, 8 tomato seedlings were examined and counted to calculate the percentage of dead plants. Means and standard errors were calculated from nine independent experiments. Asterisks indicate significant difference (Student's *t*-test, $P < 0.05$).

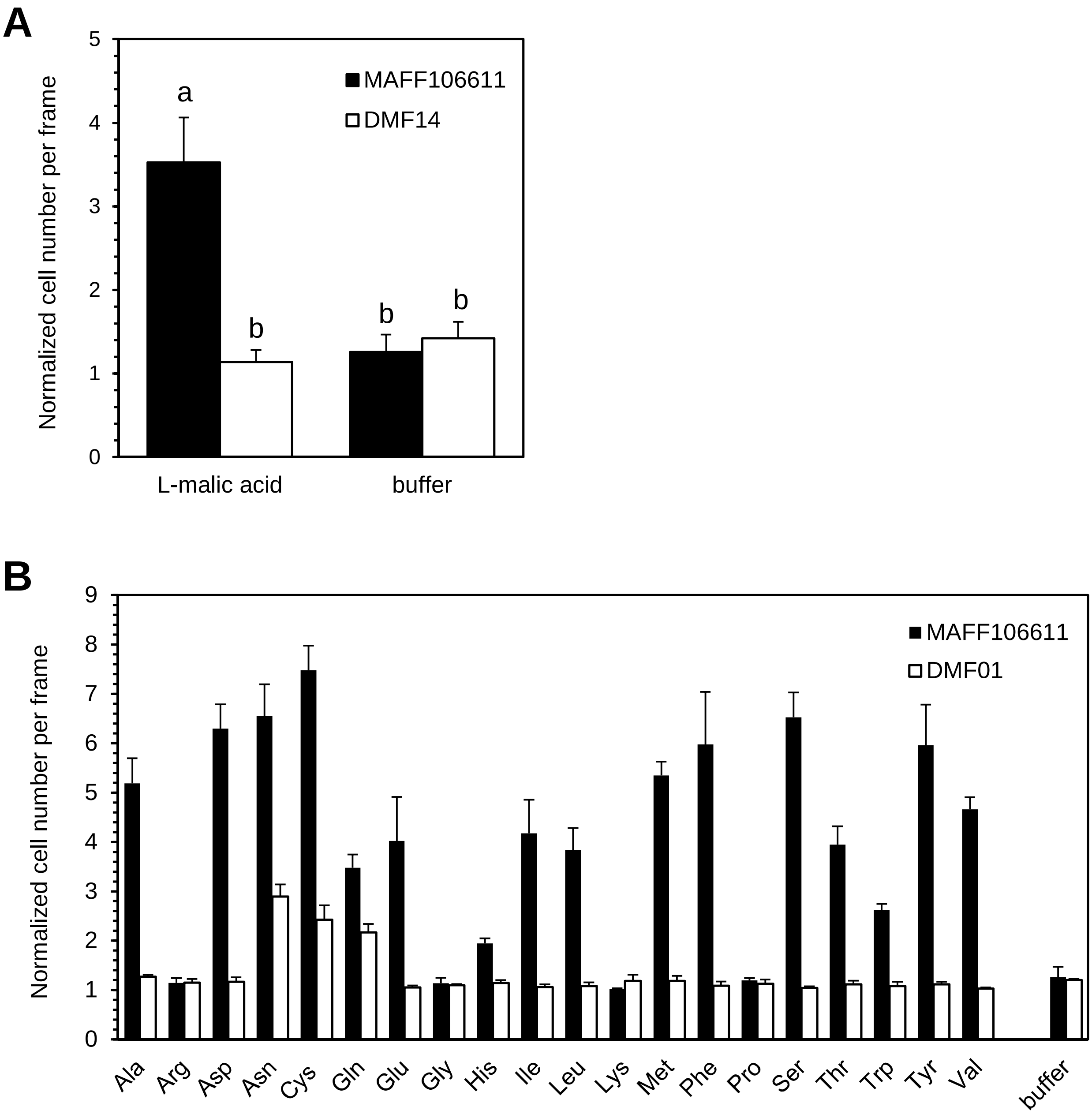

**Fig. S3** Chemotactic responses toward L-malate and amino acids by *R. pseudosolanacearum* MAFF106611 wild-type strain and mutants. Bacterial cells were grown for 20 h in RSM medium. Videotape frames were analyzed at the initiation of observation and 2 min after the initiation. Normalized cell numbers were calculated by dividing the number of bacterial cells at 2 min by that at the initiation of the observation. Buffer indicates 10 mM HEPES buffer as negative control. **A**, Chemotactic responses to 5 mM L-malate by *R. pseudosolanacearum* MAFF106611 wild-type strain and *mcpM* deletion mutant (DMF14). Different letters indicate significant difference (Student's *t*-test, $P < 0.05$). **B**, Chemotactic responses to 5 mM naturally-occurring amino acids by *R. pseudosolanacearum* MAFF106611 wild-type strain and *mcpA* deletion mutant (DMF01). There are significant differences in chemotaxis toward amino acids other than Arg, Gly, Lys, and Pro between wild-type strain and DMF01 (Student's *t*-test, $P < 0.05$). Vertical bars represent the standard errors of measurements done at least triplicate.

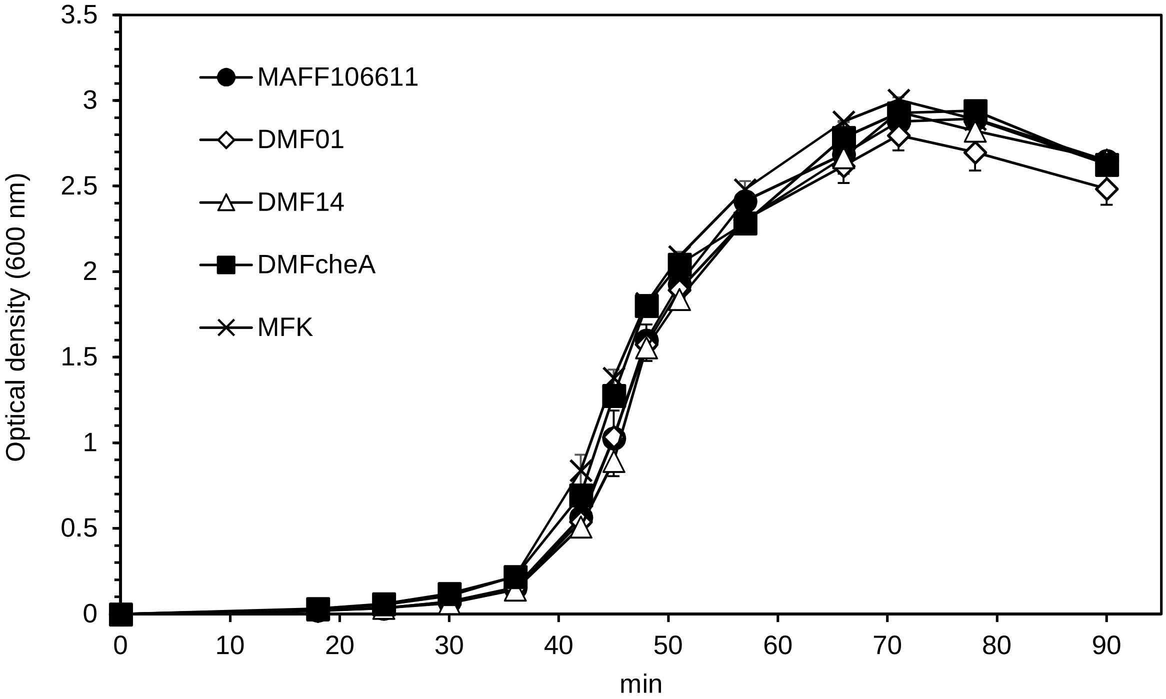

**Fig. S4** Growth of *R. pseudosolanacearum* MAFF106611 wild-type strain and mutants in PNS medium containing 5 g/l glucose. Wild-type strain MAFF106611, *mcpA* deletion mutant (DMF01), *mcpM* deletion mutant (DMF14), *cheA* deletion mutant (DMFcheA), and kanamycin-resistant strain (MFK) were tested. Vertical bars represent the standard errors of measurements done in triplicate. There were no significant differences in growth between wild-type strain and mutants (Student's *t*-test, $P < 0.05$).

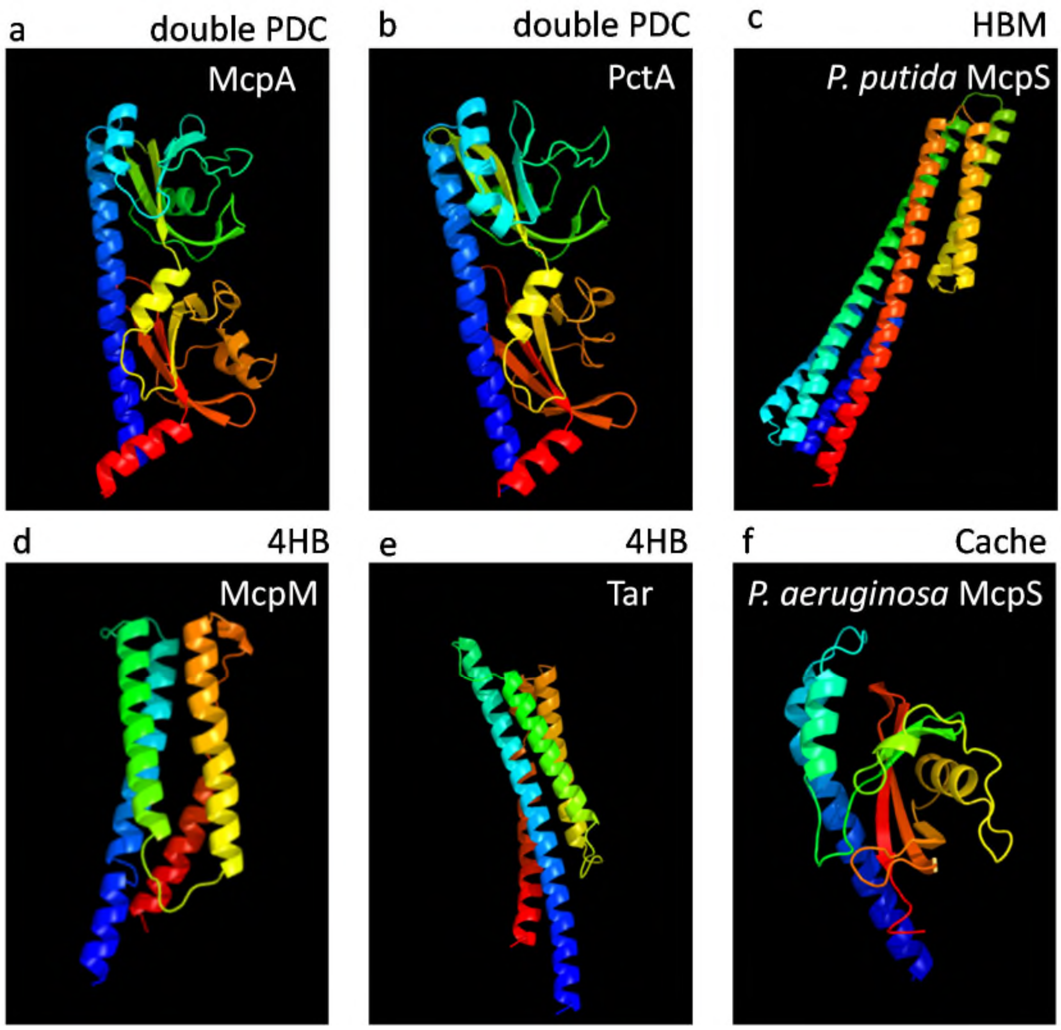

**Fig. S5** The predicted three-dimensional (3D) structures of LBDs of bacterial MCPs. Protein structure ribbon 3D models of (a) *R. pseudosolanacearum* Ps29 McpA, (b) *P. aeruginosa* PAO1 PctA, (c) *P. putida* KT2440 McpS, (d) *R. pseudosolanacearum* Ps29 McpM, (e) *E. coli* Tar, and (f) *P. aeruginosa* PAO1 McpS. 3D structures of MCP LBDs were predicted by using Phyre$^2$ algorithm (1) (Phyre2 sever: http:://www.sbg.bio.ac.uk/phyre2). Blue color, N-terminus; red color, C-terminus.

## Reference

1. **Kelley LA, Mezulis S, Yates CM, Wass MN, Sternberg MJ.** 2015. The Phyre2 web portal for protein modeling, prediction and analysis. Nat Protoc **10:**845-858.